Rib waveguides for trapping and transport of particles

Balpreet Singh Ahluwalia,* Øystein Ivar Helle, and Olav Gaute Hellesø

[1]*Department of Physics and Technology, University of Tromsø, 9037 Tromsø, Norway*
**balpreet.singh.ahluwalia@uit.no*

Abstract: Rib waveguides are investigated as an alternative to strip waveguides for planar trapping and transport of microparticles. Microparticles are successfully propelled along the surface of rib waveguides and trapped in the gap between opposing rib waveguides. The trapping capabilities of waveguide end facets formed by a single and opposing waveguide geometries are investigated. The slab beneath a rib waveguide continues to guide light after the end facet of a rib waveguide. Thus particles can be trapped in wider gaps formed by opposing rib waveguides than with strip waveguides. Rib waveguides were found more efficient in trapping a collection of particles in the gap and particles could be moved to different locations in the gap by changing the relative power in the two opposing rib waveguides. Numerical simulations are used to show that the trapping efficiency on the surface of rib and strip waveguides is comparable. The simulations also confirm the advantage of opposing rib waveguides for trapping particles in wide gaps. The low sidewalls of rib waveguides give low propagation losses and make it easy to integrate rib waveguides with other functions in a lab-on-a-chip where particle trapping and transport is required.

OCIS codes: (130.3120) Integrated optics devices; (350.4855) Optical tweezers or optical manipulation; 230.7370 Waveguides.

References and links

1. O. M. Maragò, P. H. Jones, P. G. Gucciardi, G. Volpe, and A. C. Ferrari, "Optical trapping and manipulation of nanostructures," Nature Nanotechnol. **8**, 807–819 (2013).
2. D. G. Grier, "A revolution in optical manipulation," Nature 424(6950), 810–816 (2003).
3. S. Kawata and T. Tani, "Optically driven Mie particles in an evanescent field along a channeled waveguide," Opt. Lett. **21**, 1768–1770 (1996).
4. B. S. Ahluwalia, P. McCourt, T. Huser, and O. G. Hellesø, "Optical trapping and propulsion of red blood cells on waveguide surfaces," Opt. Express 18, 21053–21061 (2010).
5. S. Gaugiran, S. Gétin, J. M. Fedeli, G. Colas, A. Fuchs, F. Chatelain, and J. Dérouard, "Optical manipulation of microparticles and cells on silicon nitride waveguides," Opt. Express 13(18), 6956–6963 (2005).
6. D. Yin, E.D. Yin, E. J. Lunt, M. I. Rudenko, D. W. Deamer, A. R. Hawkins, and H. Schmidt, "Planar optofluidic chip for single particle detection, manipulation, and analysis," Lab Chip **7**, 1171–1175 (2007).
7. A. H. J. Yang, S. D. Moore, B. S. Schmidt, M. Klug, M. Lipson, and D Erickson, "Optical manipulation of nanoparticles and biomolecules in sub-wavelength slot waveguides," Nature **457**, 71 (2009).
8. S. Kühn, P. Measor, E. J. Lunt, B. S. Phillips, D. W. Deamer, A. R. Hawkins, and H. Schmidt, "Loss-based optical trap for on-chip particle analysis," Lab Chip **9**, 2212–2216 (2009).
9. P. T. Lin, H. Y. Chu, T. W Lu, and P. T. Lee, "Trapping particles using waveguide-coupled gold bowtie plasmonic tweezers," Lab Chip **14**, 4647–4652 (2014).
10. S. Gaugiran, S. Gétin, G. Colas, A. Fuchs, F. Chatelain, J. Dérouard, and J. M. Fedeli, "Optical manipulation of microparticles and cells on silicon nitride waveguides," Opt. Express **13**, 6956–6963, (2005).
11. Ø. I. Helle, B. S. Ahluwalia, and O. G., Hellesø, "Optical transport, lifting and trapping of micro-particles by planar waveguides," Opt. Express **23**(5), 6601–12 (2015).
12. O. G. Hellesø, P. Løvhaugen, A. Z. Subramanian, J. S. Wilkinson, and B. S. Ahluwalia, "Surface transport and stable trapping of particles and cells by an optical waveguide loop," Lab Chip **12**, 3436–3440 (2012).

13. B. S. Ahluwalia, A. Z. Subramanian, O. G. Hellesø, N. M. B. Perney, N. P. Sessions, and J. S. Wilkinson, "Fabrication of submicrometer high refractive index Tantalum Pentoxide waveguides for optical propulsion of microparticles," IEEE Photonic Tech. L. **21**(19), 1408–1410 (2009).
14. B. S. Ahluwalia , P. McCourt, A. Oteiza, J.S. Wilkinson, T. R. Huser, and O. G. Hellesø, "Squeezing red blood cells on an optical waveguide to monitor cell deformability during blood storage," Analyst **140**(1), 223–9, (2015).
15. S. Lindecrantz and O. G. Hellesø, "Estimation of propagation losses for narrow strip and rib waveguides," IEEE Photonic Tech. L. **26**, 1836–1839 (2014).
16. G. P. McNerney, W. Hübner, B. K. Chen, and T. Huser, "Manipulating CD4+ T cells by optical tweezers for the initiation of cell-cell transfer of HIV-1", J. Biophotonics **3**(4), 216–223 (2010).
17. B. Agnarsson, S. Ingthorsson, T. Gudjonsson, and K. Leosson, "Evanescent-wave fluorescence microscopy using symmetric planar waveguides," Opt. Exp. **17(**7), 5075–5082 (2009).
18. B. Agnarsson, A. B. Jonsdottir, N. B. Arnfinnsdottir, and K. Leosson, "On-chip modulation of evanescent illumination and live-cell imaging with polymer waveguides," Opt. Exp. **19**, 22929–22935 (2011)
19. A. Dhakal, A. Raza, F. Peyskens, A. Subramanian, S. Clemmen, N. Le Thomas, and R. Baets, "Efficiency of evanescent excitation and collection of spontaneous Raman scattering near high index contrast channel waveguides," Opt. Exp. **23**, 27391, (2015).
20. L. C. Hsu, T. C. Chen, Y. T. Yang, C. Y. Huang, D. W. Shen, Y. T. Chen, M. C. M. Lee, "Manipulation of micro-particles through optical interference patterns generated by integrated photonic devices," Lab Chip **13**, 1151–1155 (2013).
21. M. C. Estevez, M. Alvarez, L. M. Lechuga, "Integrated optical devices for lab-on-a-chip biosensing applications," Laser Photonics Rev. **6**, 463–487 (2012).
22. B. S. Phillips, P. Measor, Y. Zhao, H. Schmidt, and A. R. Hawkins, " Optofluidic notch filter integration by lift-off of thin films," Opt. Express **18**(5), 4790–4795, (2010).

1. Introduction

Optical trapping has found a number of applications in biology and nanotechnology [1-2]. Optical waveguides made with a thin layer of a high refractive index material give a strong evanescent field. It has been shown that this evanescent field can successfully trap and propel a range of particle types (polystyrene spheres, nanowires, cells, virus) and sizes [3-14]. Different waveguide geometries have been employed, such as diffused [3], strip [4-6, 10-14], slot [7], ARROW [8] and plasmonic [9] waveguides. Narrow rib waveguides have significantly lower propagation losses than strip waveguides due to the lower side-walls [15]. In this work, a systematic study of rib waveguides for planar waveguide trapping, and in comparison with strip waveguides, is presented. The lower propagation losses can make it possible to propel particles over longer distances and thus use optical trapping in larger lab-on-a-chip systems.

The evanescent field on the surface of planar waveguides can be used to trap particles in two dimensions. By designing the waveguide to end, the light diverging out from the waveguide facet can also be accessed for optical trapping applications [12]. At the end facet of a strip waveguide, the field ceases to be guided and the output beam diverges fast. Using the field in the gap between end facets from two opposing waveguides, particles can be stably trapped and also lifted up in three-dimensions away from the surface [11-12]. However, it is shown in this paper that when the gap between the end facets of strip waveguides increases (>20 μm), the trapping capabilities are reduced significantly. A rib waveguide can be described as a narrow rib on top of a wide slab waveguide. Thus, at the end of a rib waveguide, there is a slab waveguide that continues to the edge of the chip. It will be shown that this slab waveguide gives significantly reduced divergence at the end of the rib, as compared to the end of a strip waveguide. This is taken advantage of to trap particles in up to 50 μm wide gaps between opposing rib waveguides, which is not possible between strip waveguides. Trapping in a wide gap makes it possible to collect a number of particles in an area.

In this article, optical trapping at the surface of rib waveguides, after the end and in the gap between end-facets from opposing rib waveguides will be studied and compared with trapping by similar strip waveguide structures. The effects are demonstrated experimentally,

while numerical simulations are used to study the optical forces as function of the geometrical parameters of the waveguides.

2. Methods

2.1 Waveguide design and fabrication

Strip and rib waveguides are shown schematically in Figs. 1 (a) and 1(c). For strip waveguides, the guiding layer is completely etched down to the under-cladding, while for rib waveguides, it is only partially etched down. The strip waveguide gives tighter horizontal confinement than the rib, as shown by the mode profiles in Figs. 1(b) and 1(d). Vertically, the extent of the evanescent field into the top-cladding (here: water) is approximately the same. It is easier to make single-mode waveguides with the rib-structure than with strip due to weaker horizontal guiding. The roughness of the etched sidewalls is the main sources of propagation losses, and as the sidewalls are lower for rib-waveguides, they have lower propagation losses as compared to strip waveguides of similar geometry [15].

To compare optical trapping with the two types of waveguides, both strip and rib waveguides were made. For both types, a 180 nm thick core layer was deposited with sputtering of tantalum pentoxide (Ta_2O_5) on thermally grown silica on a silicon wafer. Ion-milling was used to etch the core completely down to the silica for the strip waveguides, and 50 nm down for the rib waveguides, see Fig. 1. The width of the waveguides was 1.3 µm. Further details on the fabrication are given in [13]. Ta_2O_5 was chosen for the core due to its high refractive index (2.15 at 1070 nm wavelength). Combined with the thin core layer, this gives a strong evanescent field, which is essential for optical trapping.

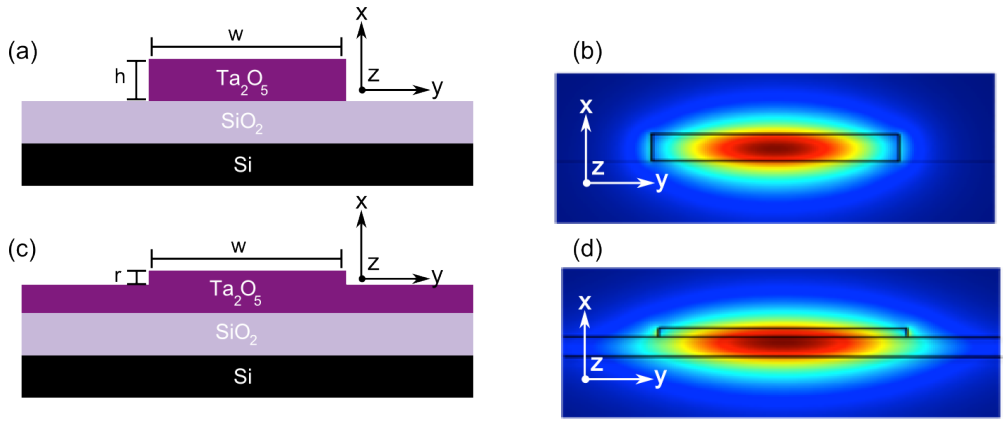

Fig. 1: Schematic diagram of a) strip waveguide with strip height (h) of 180 nm and b) its fundamental TE-mode. c) shows a rib waveguide with rib height (r) of 50 nm and d) its fundamental TE-mode. Both waveguides have a width (w) of 1.3µm. Figure not drawn to scale.

In addition to studying optical trapping on top of waveguides, optical forces from a single end facet of a waveguide and in the gap between two waveguide end facets are also investigated, as outlined in Fig. 2. The waveguide was split in two with a Y-junction and the two arms were curved to form a loop structure. The waveguide ends and gaps were defined with photolithography, and were located in the middle of the loop structure, see Fig. 2(e). A similar structure has previously been used to trap particles in a 2 µm wide gap [12] and to lift particles [11], both using strip waveguides.

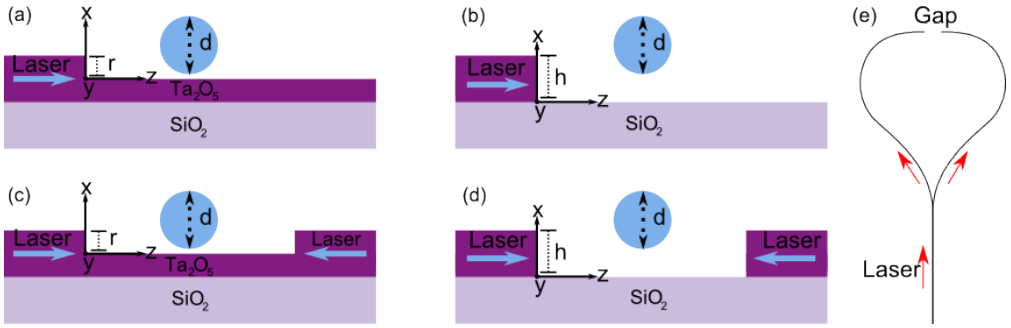

Fig. 2: Outline of the waveguide ends used in this work. A single end facet is compared for a) rib and b) strip waveguides. Two opposing waveguide end facets are also analyzed for c) rib and d) strip waveguides. e) The opposing waveguide end facets are formed a by loop with a gap in the middle. A sphere is shown with diameter d and distance z from the waveguide end. The core height is kept constant at h = 180nm for rib and strip waveguides. The rib height (r) was 50 nm for the experiments with rib waveguides, while it was used as a variable for the simulations. Figure not drawn to scale.

2.2 Experimental set-up

Light was end-coupled into the waveguides. The light source was a 5W Ytterbium fiber laser at 1070 nm wavelength and it was coupled in using an IR-coated long working distance objective lens (100X, 0.8 N.A). Piezoelectric translation stages were used to align the objective and the waveguide chip. The waveguide chip was kept on a vacuum chuck to avoid any mechanical drift. An upright microscope equipped with long working distance 20X and 50X objective lenses (20X NA0.4 and 50X NA0.8) and a CCD camera was employed to acquire images. A diagram of the experimental set-up is given in [4]. The input power for all the experiments was kept in the range of 300-500 mW. The propagation losses were experimentally measured for rib and strip waveguides in [15] to be 1.7 dB/cm and 6.7 dB/cm, respectively, for 785 nm. As the rib height was larger in this work (50nm vs. 20 nm in [15]), the propagation losses for the rib waveguide are estimated to be approximately 3 dB/cm. Also, the thickness of the strip waveguide used in this work was smaller (180 nm vs. 220 nm in [15]), the propagation losses for the strip waveguide are estimated to be 6.2 dB/cm. Thus, propagation losses are approximately twice as large for the strip as for the rib waveguides used in this work.

2.3 Simulations

The electromagnetic field distribution of different waveguide designs and particles was simulated with Comsol. To determine the optical forces on a particle, Maxwell's stress tensor was integrated over the surface of the particle. The particles were taken to be spherical with a diameter of 1 and 3μm, and with a refractive index of 1.59, corresponding to polystyrene. The sphere was positioned at different locations in the model (xz-plane, axis defined in Fig. 1 and 2) and the field and forces calculated for each location. Only positions in the xz-plane going through the centre of the waveguide (y = 0) were considered. This makes the model symmetric about the y-axis, making it possible to simulate only half the model. This reduced the size of the model. For the gap, the model is also symmetric about the centre of the gap (z = gap/2). Thus, forces were only computed up to this point. The model was computationally intensive due to the large gap simulated (10 μm). A computer cluster was used to run the model. The total guided power in the waveguides was set to 1 mW and the forces scaled with this value. For a single waveguide, the power was thus set to 1 mW, while for a gap, the power in each waveguide was set to 0.5 mW.

3 Results

3.1 Experimental results

We first studied optical trapping on a straight rib waveguide. Polystyrene spheres of diameter 1-5 μm and red blood cells were successfully trapped and propelled by the rib waveguide along the pre-fabricated path, which included straight, Y-junctions and bend geometries. Visualization 1 shows waveguide trapping and propulsion of red blood cells by a rib waveguide. The cells were submerged in isotonic sucrose medium (0.25 molar, [4]). The laser power incident on the waveguide was 500 mW. This demonstrates that rib waveguides can indeed be used for trapping and propulsion of microparticles. Squeezing of red blood cells has previously been demonstrated on strip waveguides [14], but this was not tested for the rib waveguides.

Next, 3 μm particles were trapped in a 20 μm wide gap between opposing end facets of rib waveguides and the results were compared against identical experiments using opposing end facets formed by strip waveguides. Fig. 3(a) and visualization 2 shows optical trapping of microparticles in a gap between opposing rib waveguides. The movie starts with a particle trapped in the gap. Subsequently, more particles are trapped on top of one of the waveguides and are propelled into the gap, where they are trapped stationary. This shows that a single or a group of particles can be stably trapped in a relatively large gap between rib waveguides. To compare, Fig. 3(b) and visualization 3 shows trapping in the gap between opposing strip waveguides. The movie shows two 3 μm particles entering a 20 μm gap, but both particles are knocked out of the gap as they approach the center and no stable trapping is observed. The second particle moves slightly upwards (becomes out of focus) just before it is knocked out of the trap. Contrary to the rib waveguides, the trapping of particle in a 20 μm gap (and larger) formed by opposing strip waveguides was unsuccessful.

The multi-mode nature of the waveguides made it possible to change the trapping position in the gap between rib waveguides, by changing the relative power incident from the two sides. Horizontally translating the input objective with respect to the waveguide input facet is sufficient to change the intensities guided inside the two waveguide arms. A large change in the relative power between the two arms was possible, such that all the particles were guided towards one arm and the propulsion along the other arm seized (see Visualization 4). Figure 4 and visualization 5 and 6 show the feasibility to move the location of 1 and 3 μm diameter particles in a 20 μm gap. In Visualization 5, a group of 1 μm particles are trapped and manoeuvred along the gap by changing the relative guided power between the two waveguides. We observed that 1 μm particles tend to clump together near the centre of the gap. At the end of a rib waveguide, light diverges slowly, allowing particles to clump together. We have also tested optical trapping of 1 and 3 μm particles in a 50 μm gap and achieved similar results.

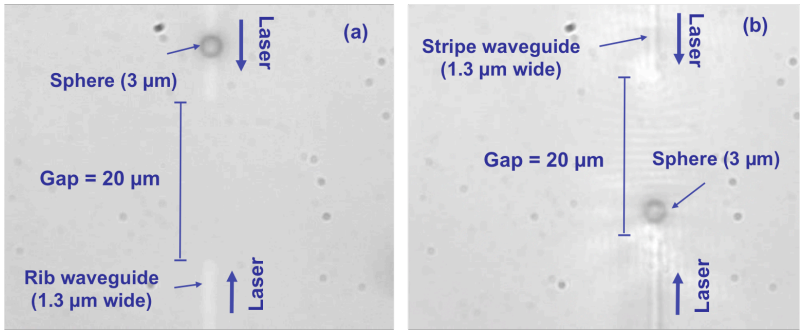

Fig. 3: Optical trapping of 3 μm diameter particles in a 20 μm wide gap between opposing waveguides for a) rib and b) strip geometries, respectively (visualization 1, 2, 3)

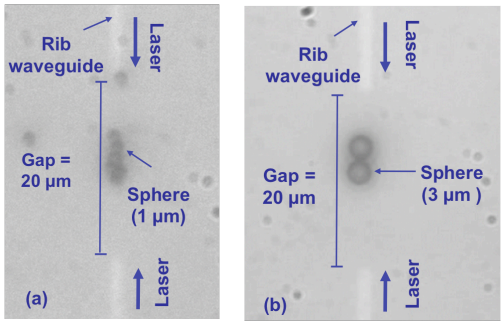

Fig. 4: Moving trapped particles of diameter a) 1 µm and b) 3 µm in a 20 µm wide gap between two rib waveguides (visualization 4, 5, 6).

3.2 Simulation results

3.2.1 Field distribution

The fundamental modes of strip and rib waveguides were found as shown in Figs. 1(b) and 1(d) for the parameters given in Figs. 1(a) and 1(c). The power in the evanescent field was found to be 10.8% and 11.2% of the guide power for rib and strip waveguides, respectively, for the fundamental mode. The fundamental mode of a rib waveguide extends further horizontally, into the adjacent slab region, than that of a strip waveguide. Thus, as the mode is wider, it is expected that the intensity in the rib is smaller than in the strip waveguide, both in the core and in the evanescent field. However, for the thin and narrow waveguides employed here, this effect is small as shown by the small difference in power in the evanescent field.

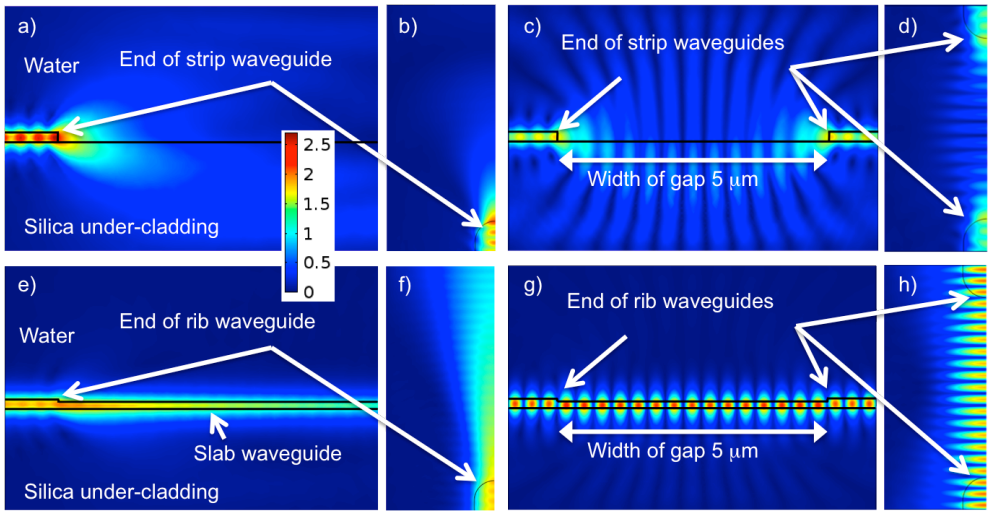

Fig. 5: Simulated field distributions at the end of strip and rib waveguides and in the gap between waveguides. The normalized electric field is shown with the same color scale and for the same total input power (1 mW) for all distributions. The fields shown are a) side-view of end of strip waveguide, b) top-view of end of strip waveguide, c) side-view of gap between strip waveguides, d) side-view of gap between strip waveguides, e) side-view of end of rib waveguide, f) top-view of end of rib waveguide, g) side-view of gap between rib waveguides and h) top-view of gap between rib waveguides. Normalized electric field (10^6 V/m).

Simulations were carried out to study light divergence from the end facet of strip and rib waveguides, and in the gap between two opposing waveguides. The resulting field distributions are shown in Figure 5. The light emitted from the end of a strip waveguide diverges fast see Figs. 5(a) and 5(b). The intensity thus decreases fast away from the end of the waveguide. At the end of a rib waveguide light is vertically guided in the slab. Thus, the light only diverges horizontally, see Figs. 5(e) and 5(f). As a consequence, the intensity after the end of the waveguide decreases much slower than for the strip waveguide. Some light is reflected at the end of the strip waveguide see Fig. 5(a), creating interference fringes between the incident and the reflected waves inside the waveguide. On the other hand, the reflection from the end of the rib waveguide is very small (due to the small rib height) and thus the interference fringes are hardly visible inside the rib waveguide see Fig. 5(e).

Regarding the field in the gap between two opposing waveguides see Figs. 5 (c), 5(d), 5(g) and 5(h), the counter-propagating beams create interference fringes. Due to the fast divergence at the end of the strip waveguide, the intensity of the interference fringes decreases much faster into the gap with opposing strip waveguides than with opposing rib waveguides. For opposing strip waveguides, the intensity in the center of the gap is thus strongly influenced by the width of the gap. This limits the trapping capabilities of opposing strip waveguides for large gap widths as observed experimentally and found by the simulation results discussed below.

3.2.2 Optical forces on top of rib a waveguide

Experimentally, rib waveguides were used to trap particles and red blood cells. To further investigate the trapping capabilities of rib waveguides, a simulation model was made to compute optical forces on a 1 μm sphere on top of a waveguide as shown in Fig. 6. The forces are computed as function of rib height (r), with the strip waveguide as a limiting case (rib height = core height). For the rib height of 50 nm used experimentally in this work, the vertical force (F_x) is about 20% less than for a strip waveguide, while the forward force (F_z) is approximately 10% less than for a strip waveguide. This supports the experimental findings that rib waveguides are suitable for optical trapping. For rib heights of less than 50 nm, the forces decrease more rapidly with decreasing rib height. However, optical trapping with a rib height of 5 nm has been demonstrated for a core height of 150 nm, showing that shallow rib waveguides can also be used for trapping.

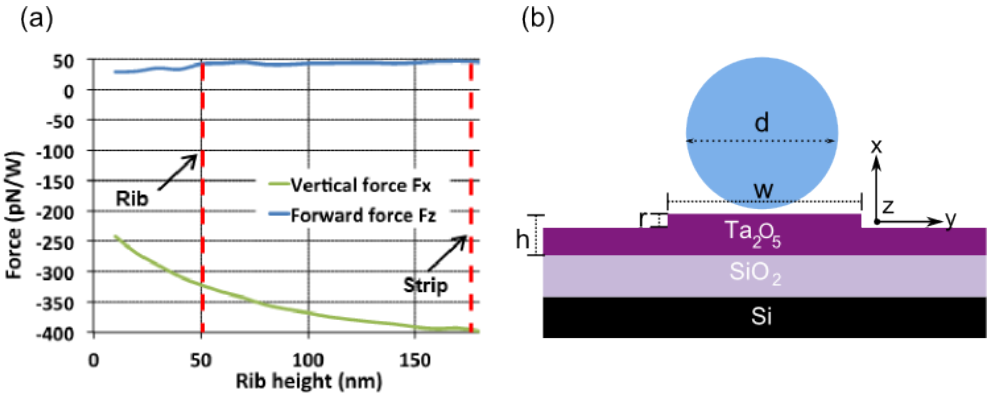

Fig. 6 (a) Vertical (F_x) and forward (F_z) optical forces on a 1 μm diameter (d) particle trapped on top of a rib waveguide with a width (w) of 1.3 μm as function of rib height (r), with a constant core height (t) of 180 nm. The dashed red vertical lines show r = 50 nm and r = 180 nm, corresponding to respectively the rib and strip waveguides used experimentally. (b) Schematic diagram to illustrate the simulation parameters of a). Figure not drawn to scale.

3.2.3 Optical forces from the end facet of a rib waveguide

The optical forces at the end of a waveguide were simulated with a 1 µm sphere fixed at z = 5 µm from the end of the waveguide. Fig. 2(a) depicts the simulation case. The forces were computed as a function of the rib height, as shown in Fig. 7. Again, the strip waveguide is a limiting case (rib height = core height of 180 nm). At the end of a waveguide, the emitted light diverges fast and the intensity decreases, as shown in Figs. 5(a) and 5(e). The optical forces decrease rapidly as the rib height increases beyond 100 nm. The maximum forces are found for a rib height of r = 70 nm for the case considered here. This optimum rib height depends on the position and size of the sphere, and the forces are always decreasing away from the end of the waveguide as discussed below (Fig. 8).

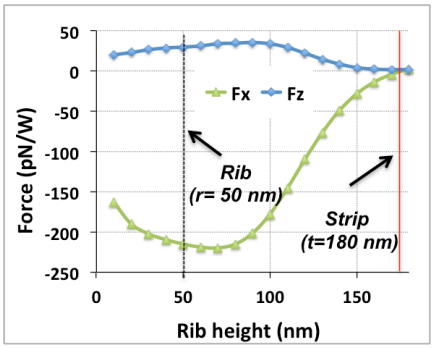

Fig. 7 Vertical (F_x) and forward (F_z) optical forces on a 1 µm diameter (d) particle located 5 µm away from the end of the waveguide, as function of rib height (r). The core height is kept constant at 180 nm. The dotted and straight lines show rib waveguide with r = 50 nm and strip waveguide with r = 180 nm used in the experiments.

3.2.4 Comparison of optical forces from the end facet of rib and strip waveguides

The optical forces at the end of rib and strip waveguides see Figs. 2(a) and 2(b) were compared, see Fig. 8, for 1 and 3 µm particles as function of z, i.e. displacement from the end of the waveguide. The parameters of waveguide used in the simulation were total height of 180 nm and rib height of 50 nm.

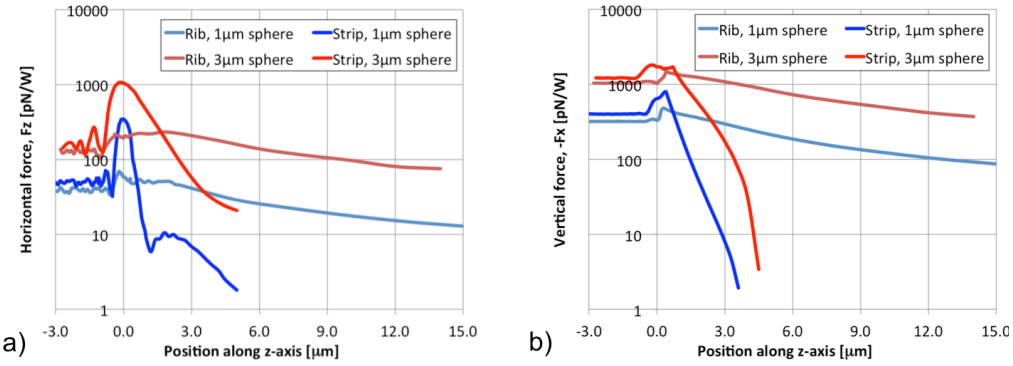

Fig. 8 (a) Forward (F_z) and (b) vertical (F_x) optical forces on 1 and 3 µm particle as a function of z position after the end of the waveguide, for rib and strip waveguides. Note logarithmic y-axis and negative F_x-values to allow logarithmic axis. The end facet of the waveguide is located at z = 0, particle is on top of waveguide surface for z < 0 and it enters the gap for z =0.

The simulation starts from negative z positions, i.e. when the particle is on top of the waveguide surface. Both rib and strip waveguides propel the particle towards the end facet (z= 0). When the particle arrives at the end of the waveguide (0<z < 2 μm), a strip waveguide imparts higher forces (both F_x and F_z) compared to a rib waveguide on a 1 and 3 μm particles. This results in an initial push for particles entering the gap of the strip waveguide (also observed experimentally, see Visualization 3). For rib waveguides, this effect is weaker. The optical manipulation capabilities of the end facets formed by a strip waveguide are thus limited to short distance (or short gaps). On the other hand, at the end of a rib waveguide, the decrease in optical forces is relatively slow as the field only diverges horizontally. As a consequence, the optical forces are still relatively large on particles located far from the end facet of rib waveguides, e.g. 25-50 μm away.

3.2.5 Optical forces in the gap between opposing rib waveguides

Simulations were done to study the trapping capabilities of opposing rib waveguides. Experimentally, particles were trapped in a 20 μm wide gap between rib waveguides. To show the principle, while limiting the size of the simulations, forces were calculated on 1 and 3 μm spheres in a 10 μm wide gap. Light is incident from both waveguide ends, as shown in Fig. (2c). The calculated forces are shown in Fig. 9 as function of the position of the spheres in the gap. Due to the symmetry, forces were calculated only for the first half of the gap. The forward force (F_z) is anti-symmetric about the centre of the gap, thus positive for z< 5 μm and negative for z > 5 μm, resulting in a push towards the center of the gap (z = 5 μm) where F_z = 0. The vertical force (F_x) is symmetric about the centre and thus negative throughout the gap. The particle is thus attracted downwards to the waveguide. For F_z, oscillations are visible that resembles interference fringes. The two counter-propagating beams give interference fringes, see Fig. 5, that are separated by $\lambda_0/2n_{eff}$ = 315 nm, where n_{eff} is the effective refractive index of the guided mode. For positions 3 μm < z < 4 μm, the period of the oscillations in F_z is close to this value for 1 μm spheres. For 3 μm spheres, the oscillations match the interference period for 3.5 μm < z < 4.5 μm. Further away from the centre, z < 3 μm, the oscillations are less periodic and the spacing does not match the interference period. The power in the two counter-propagating beams will be different further from the centre of the gap and it is also possible that the interaction between the waveguide end and the sphere becomes significant, thus reducing the effect of interference.

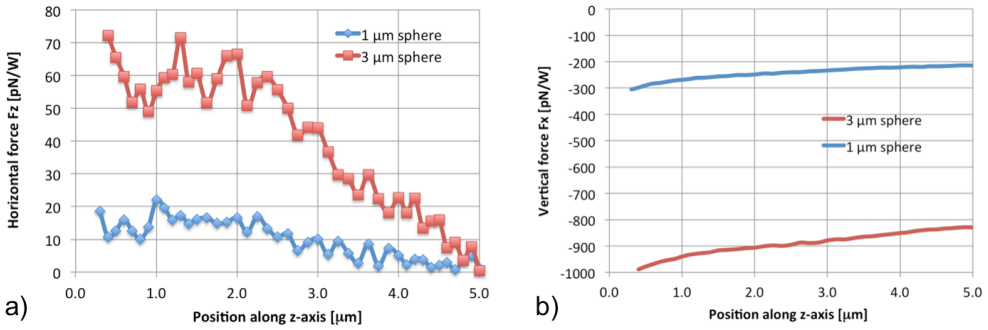

Fig. 9 (a) Forward (F_z) and (b) vertical (F_x) optical forces on 1 and 3 μm particles in the gap between two opposing rib waveguides. The displacement is from the end of the left waveguide to the center of the sphere. F_z is anti-symmetric and F_x symmetric about the centre of the gap (z = 5 μm), such that z >5 μm gives $F_z(z)= -F_z(10\mu m - z)$ and $F_x(z)=F_x(10\mu m - z)$.

4. Discussion and conclusions

In this paper, we show that rib waveguides provide an alternative design option for optical trapping and transport of particles. It was found that the power in the evanescent field

of a rib waveguide is almost identical to that of a strip waveguide for the parameters used here. The forces on a particle in the evanescent field were also similar for the two waveguide geometries. For trapping and propulsion over relatively large distances, the low propagation losses give the rib waveguide an advantage. The rib geometry also has an advantage over the strip geometry when considering forces on particles after the end of the waveguide, and in the gap formed by opposing waveguides. A rib waveguide consists of the rib and a slab waveguide, with the slab waveguide continuing to the edges of the chip. Thus, at the end of the rib, light continues to be guided in the slab. This gives vertical guiding, while the light diverges horizontally. Thus, the intensity decreases more slowly than after the end of a strip waveguide (Fig. 8). This can be used to propel particles away from the end or to trap particles in a wide gap between opposing rib waveguides. It was shown experimentally that particles (1-3 μm) could be trapped in a gap as wide as 50 μm. For a large gap, such as 50 μm, particles can also be accumulated at the center of the gap for rib waveguides. This is because of the divergence of the light guided in the slab, for rib waveguides see Fig. 5(b). Another advantage of rib waveguides is the possibility of moving particles in the gap. By changing the relative power in the two waveguide arms leading to the gap, the stable trapping location can easily be altered. Experimentally, this was shown with 1 and 3 μm particles, both for single particles and a collection of particles.

A 10 μm gap between strip waveguides was previously shown to optically lift and stably trap 1-3 μm diameter particles [11]. However, for gaps with larger separation, the optical forces from the end of a strip waveguide decrease rapidly with distance in accordance with the rapid divergence of the field (Fig. 5), thus not giving stable trapping as shown experimentally (Fig. 3).

The simulations suggest an extra push to the particles as they enter the gap (Fig. 8), and this was also observed experimentally (Visualization 2, 3). The strip waveguide gives an initial push in the z-direction mainly because the particle falls down (to $x = 0$) and is illuminated by the output light (from end facet of waveguide) rather than the evanescent field. The forward force (F_z) oscillates in the gap (Fig. 9) because of the interference of counter-propagating beams, the interaction between particles and beam and possibly also with the waveguide ends.

The capability to trap multiple particles in a relatively large gap between rib waveguides, will be useful to bring two or more cells in close vicinity to initiate cell-to-cell interactions [16] or to study the influence on the cells of chemical or biological substances. As the trapped particles or cells are kept in close contact with the surface, a wide gap is also suitable for studying interactions with the surface. The superiority of a rib over a strip waveguide in terms of propagation losses will also be useful in waveguide chip-based microscopy [17], live cell-imaging [18] and waveguide chip-based Raman spectroscopy [19].

With low propagation losses and by combining confinement and divergence, rib waveguides are promising for integration in lab-on-a-chip systems [20-22] where particle trapping and manipulation is required. By tuning the waveguide geometry to the exact application, the performance can be optimized while requiring a single lithographic step. Also, due to the low sidewalls, it is easy to combine them with other functions, e.g. microfluidic [22]. The divergence of the light at the end of the waveguide can also be changed by tuning waveguide width, slab thickness and rib height, thus controlling the divergence of the optical forces away from the end and across a gap.

Acknowledgments

The authors thank James S. Wilkinson, Peter McCourt and Ananth Z. Subramanian for their help. Acknowledgment to the European Research Council (ERC) Grant (Project No 336716, “Nanoscopy”).